A Micro-scale Wind Turbine Fed BLDC Motor for Electric Vehicle Drive Application

Saeed Masoumi Kazraji*‡, Saheb Khanabdal*, Ramin Bavil Soflayi*, Mehran Sabahi*

*Faculty of Electrical and Computer Engineering, University of Tabriz

(masoumikazraji@tabrizu.ac.ir, s.khanabdal90@ms.tabrizu.ac.ir, ramin.bavil90@gmail.com, sabahi@tabrizu.ac.ir)

‡ Corresponding Author; Saeed Masoumi Kazraji, Faculty of Electrical and Computer Engineering University of Tabriz, Tabriz, Iran, +98 411 339 3715, masoumikazraji@tabrizu.ac.ir

Received: 21.11.2013 Accepted: 24.12.2014

Abstract- A brushless dc motor (BLDCM) based driver with a wind-generator (WG) in maximum power point tracking (MPPT) condition is proposed in this paper. In the proposed system there are a buck-type dc/dc converter, which is high efficiency type, and a control unit which is used for run the MPPT function. The WG optimal power characteristic and wind speed measuring data are not required while the WG works in variable speed mode, therefore higher reliability and simplicity of the WG are achieved, and also cost and mechanical stresses will be reduced. Moreover better usage of available wind energy is achieved, particularly while wind speeds are low.

Keywords- Brushless dc motor (BLDCM), wind generator (WG), electric vehicle, MPPT algorithm.

1. Introduction

In the recent years, renewable energy resources have been become important as pollution-free and unlimited energy supplies. The wind power generation system (WPGS) is included as one of the most effective ones, developed to capture and transfer wind energy into electric energy form. Cost-performance ratio in the most of WPGSs is considerable. Because of that, they are attractive to investment. Due to safety and small size of the small-scale WPGS, it is more suitable than the large-scale ones for urban environment. According to recent study of small wind turbine global market, made by the American Wind Energy Association in 2007 [1], the micro-scale WPGS is known as a small-scale ones and a WPGS which has capacity less than 1kW, can be used in electric vehicle drive application. Typically, it consists of wind turbine with fixed pitch angle, permanent-magnet (PM) generator, rectifier, dc converter, battery module, and a dc load. For increasing the efficiency of WPGS, using maximum power point tracking (MPPT) control algorithms are essential to regulate speed of turbine's rotor according to actual different wind velocity conditions. Basically, there are four different types of MPPT techniques, namely, the tip speed ratio (TSR) technique, the optimal torque (OT) technique [2], [3], the power mapping technique [4], [5], and the perturbation and observation (P&O) searching technique [6], [7].

Brushless DC motor (BLDCM) is an appropriate motor for electric drive designers, due to its attractive features such as high efficiency and energy saving, it can operate efficiently all over the speed range, more reliable than brushed DC motors and more efficient than AC variable frequency motors on the rated frequency. Furthermore, comparing with conventional AC and DC motors, there is an improvement on driving mileage about 20% to 50% in BLDCM, they also expand battery life by 30%.

In this paper a control system for driving BLDCM in electric vehicle is developed. The mathematical model of BLDCM is uesd. The proposed driver is combined with a wind-generator (WG) which is equipped by a MPPT system, including a buck-type dc/dc converter which is high efficiency type, and a control unit which runs the MPPT function. The proposed MPPT method does not need optimal power characteristic of WG or wind speed measuring anemometer. WG also works in variable velocity conditions. Thus, the system acts with higher reliability, lower complexity and cost, and mechanical stress on WG tends to be decrease.

Also BLDCM with new power converter topology is proposed by Krishnan and Shiyoung [12]. Four switch three phase BLDCM in low cost commercial applications is proposed by Krishnan [13]. The mentioned literature does not cope with modeling and simulation problems of buck converter fed BLDCM drive. In this study, the buck converter for using in BLDCM drive is proposed.

2. Electric Vehicle Driven Motor Analysis with Micro Scale Wind Turbine

Although battery technology has been developed, but constrains large-scale automotive application yet. Improving energy efficiency as well as driving course and proper usage of the battery with energy management are topics of electric vehicle research area. Two important items that develop the electric vehicle technology are as follows:

I) Electric motor driver, using of a suitable driver according to characteristic of the battery.

II) Electric vehicle motor, because of battery constraints, electric vehicles are used chiefly for urban traffic; the main durations of the vehicle operation are start, acceleration and braking working conditions. Therefore, the motor startup and acceleration performance, the efficiency in low-speed condition, braking and energy recovery ability, overload capability, electrical energy density and the reliability of electric vehicle motor are particularly important problems.

Based on the two points mentioned above, effects of the driven-motor are important for the electric vehicle performance, therefore, proper selection of the electric vehicles motor depends on not only to the battery discharge characteristics, it relates to the vehicles operation characteristics too.

A new strategy for using renewable energy sources such as wind turbines is installing them below the front bumper or on the car's roof as is shown in Fig.1. When the car moves along, it comes up against the air resistance. The resistance of the air mass hits turbine blades and leads to generate electricity. The produced energy is saved on the battery, and then used in BLDCM. So, energy is achieved by less fuel which needed before, and it decreases the cost.

Fig. 1. Electric vehicle with wind turbine.

3. Mathematical Model of BLDCM

The schematic module with the control unit of BLDCM is shown in Fig. 2. Actually, BLDCM is a permanent magnet AC motor,while its torque-current characteristics act similar with a DC motor, but uses electronic brushless commutation system. It is a modified PMSM with trapezoidal back-emf instead of sinusoidal [8]. There is a good point, which is the rotor position in order to follow the appropriate energizing sequence [9]. In this system, Hall effect sensors is used to sense position of the rotor, namely Hall_A, Hall_B, and Hall_C, embedded into the stator with a lag of 120º from the earlier. The rotor position is determined by using Hall sensors and then related windings are excited. Since control of BLDCM is easy, it is the choice in many applications requiring very accurate speed control [10], [11].

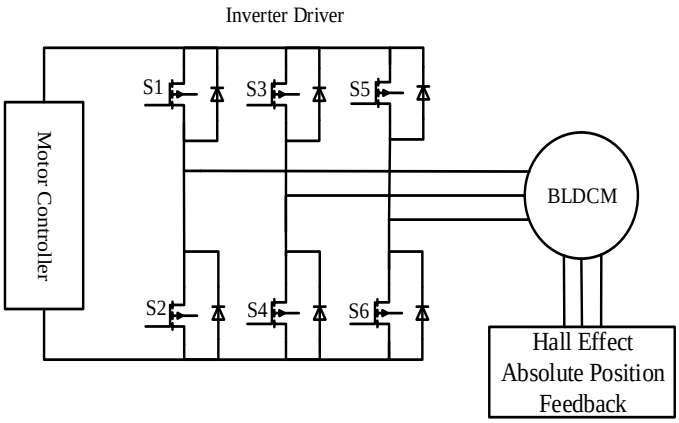

Fig. 2. The schematic module of BLDC motor.

Based on the motor model, there is a linear relationship between the electromagnetic torque T_{em} and the armature current i_a i.e., $T_{em} = k_T \cdot i_a$, where k_T is the torque factor. The back EMF in BLDCM is linearly proportioned to the rotary mechanical velocity and direction of that is determined by Flemings right hand rule. Supposing that intensity of magnetic field is *B*, length of conductor on the edge of rotor is *l*, the number of conductors in the motor is *Z* rotor radius is *r* and rotor is rotating at an angular velocity of ω_r, then the conductor's speed is given by:

$$v_{el} = r.\omega_r \tag{1}$$

The emf e in that conductor is given by:

$$e = \omega_r Bl \tag{2}$$

The emf e generated in that conductor with considering number of conductors is given by:

$$e = \omega_r Bl(Z/2) \tag{3}$$

The relationship between back EMF and angular speed of rotor is:

$$e = K_\phi \omega \tag{4}$$

Where, K_ϕ is the back EMF factor. In the model of three phases BLDCM, the summation of the phase currents has to be zero, i.e.

$$i_a + i_b + i_c = 0 \tag{5}$$

The three phase equations which are mentioned in the following, in order to model the two pole three phase BLDCM, are used:

$$\begin{bmatrix} v_a \\ v_b \\ v_c \end{bmatrix} = \begin{bmatrix} R_a & 0 & 0 \\ 0 & R_b & 0 \\ 0 & 0 & R_c \end{bmatrix} \begin{bmatrix} i_a \\ i_b \\ i_c \end{bmatrix} + \frac{d}{dt} \begin{bmatrix} L_a & L_{ba} & L_{ca} \\ L_{ab} & L_b & L_{cb} \\ L_{ac} & L_{bc} & L_c \end{bmatrix} \begin{bmatrix} i_a \\ i_b \\ i_c \end{bmatrix} + \begin{bmatrix} e_a \\ e_b \\ e_c \end{bmatrix} \tag{6}$$

The rotor field is induced by the permanent magnet, embedded in the shape of an arc, inductances of each phase be without dependence on the rotor position, hence:

$$L_a = L_b = L_c = L_p \tag{7}$$

$$L_{ab} = L_{ba} = L_{bc} = L_{cb} = L_{ca} = L_{ac} = M \tag{8}$$

Equation (6) is simplified as follows:

$$\begin{bmatrix} v_a \\ v_b \\ v_c \end{bmatrix} = \begin{bmatrix} R_a & 0 & 0 \\ 0 & R_b & 0 \\ 0 & 0 & R_c \end{bmatrix} \begin{bmatrix} i_a \\ i_b \\ i_c \end{bmatrix} + \begin{bmatrix} L_p & M & M \\ M & L_p & M \\ M & M & L_p \end{bmatrix} \frac{d}{dt} \begin{bmatrix} i_a \\ i_b \\ i_c \end{bmatrix} + \begin{bmatrix} e_a \\ e_b \\ e_c \end{bmatrix} \tag{9}$$

Reordering the earlier equations leads to equation (10):

$$\begin{bmatrix} v_a \\ v_b \\ v_c \end{bmatrix} = \begin{bmatrix} R_a & 0 & 0 \\ 0 & R_b & 0 \\ 0 & 0 & R_c \end{bmatrix} \begin{bmatrix} i_a \\ i_b \\ i_c \end{bmatrix} + \begin{bmatrix} L_p - M & 0 & 0 \\ 0 & L_p - M & 0 \\ 0 & 0 & L_p - M \end{bmatrix} \frac{d}{dt} \begin{bmatrix} i_a \\ i_b \\ i_c \end{bmatrix} + \begin{bmatrix} e_a \\ e_b \\ e_c \end{bmatrix} \tag{10}$$

4. WG Control Strategy

In this paper, in order to execute MPPT control of WG, another approach is described. Fig.3 represents the block diagram model of the proposed scheme. In this MPPT scheme, output power is monitored by using output current and voltage measurements of WG. By using the result of comparison between successive values of WG-output power, Duty cycle of the dc/dc converter is directly adjusted . Thus, knowing information about the power of WG versus the rotor speed or wind velocity characteristic is not required. WG is protected from over-speeding by using a resistive dummy load. limitations which are originated from the typical range values of wind and rotor-speed or power of the dc/dc converter do not restrict the applications of the MPPT scheme which is proposed. Although the proposed method has been modeled for an application like charging a battery with a dc/dc converter, but it is also able to use in electric vehicle drive application.

4.1. WG Strategy

The power derived from wind by the WG turbine blades, P_m, depends on the shape of the blade, the pitch angle, the radius of the rotor and its rotary velocity as follows:

$$P_m = 0.5\pi\rho C_p(\lambda,\beta)R^2V^3 \tag{11}$$

Where the air density (typically 1.25 kg/m3) is showed by ρ, the pitch angle (in degrees) is represented by β, R belongs to the blade radius (in meters), V represents the wind speed (in m/s) and $C_p(\lambda,\beta)$ is the power coefficient of wind turbine which is determined by using TSR λ. The tip-speed ratio which is represented by the term λ is, defined as:

$$\lambda = \frac{\Omega R}{V} \tag{12}$$

Where Ω (rad/s) belongs to the WG rotor velocity of rotation. If η_G is the efficiency of the generator, so the total power which is generated by the WG, *P*, will express as:

$$P = \eta_G P_m \tag{13}$$

When the blades pitch angle is equal with zero, the coefficient which belongs to the power of WG is maximized for optimum value of tip-speed ratio λ_{opt}. The characteristic curves of the WG output power under different values of wind velocity are illustrated in Fig. 4. It is obvious that for each wind velocity, there is a specific point where the output power has the its greatest value. Therefore, by controlling the load of WG in variable-velocity operation, the power which is get from the wind (MPPT control) is maximum value, continuously. TSR value almost doesn't change through all maximum power points (MPPs). This leads to a linear relationship between the rotational speed of WG and the wind velocity as follows:

$$\Omega_n = \lambda_{opt}\frac{V_n}{R} \tag{14}$$

Where Ω_n is the optimal rotational speed of WG at a wind velocity V_n.

Operation of wind turbines provides 10% to 15% higher output energy, lower mechanical stress and less power fluctuation [14]. For the variable-velocity operation,there is a disadvantage, which is requirement of a power stabilizer as the WG dummy load. However, the development in power electronics leads to the lower power-converter cost ratio and also higher levels of reliability, since the energy production gain can compensate the higher cost.

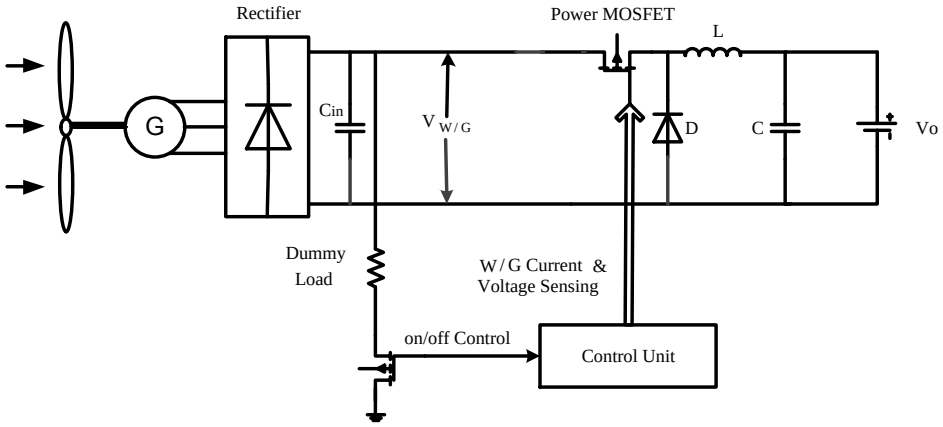

Fig. 3. Block diagram of the proposed system

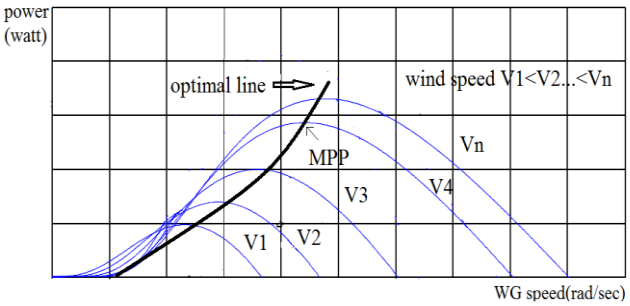

Fig. 4. WG power curves under different wind velocities.

Fig.5 shows characteristic curves of the WG torque, including the interconnected generator system/ wind-turbine, for different levels of output voltage of generator during various wind velocities. The generator is designed to act in the almost linear area, according to the straight part of the torque curves of generator in Fig. 4, for any wind-velocity situation. The point which is situated in the intersection of the turque curves of the generator and the wind-turbine, is the operating point of WG. During the MPPT efforts, applying different changes in the WG load leads to various output voltage levels of generator; thus, the generator torque is regulated in order to act at the target torque (e.g., point A) for various velocities of wind. The target-torque line related to the line which belongs to the optimal-power production is shown in Fig. 4, where the energy captured from the WG system is maximum value.

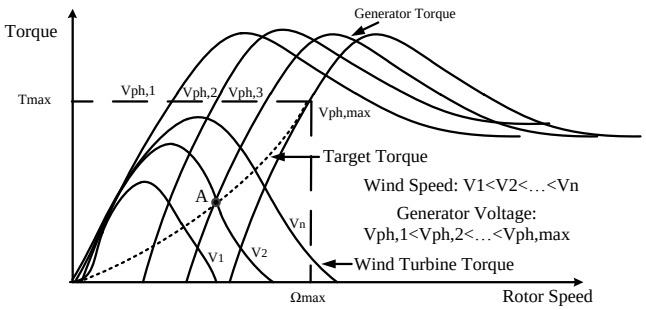

Fig. 5. Torque-speed characteristics of the wind turbine and the generator.

4.2. MPPT Algorithm

As discussed in Section I, in the MPPT process of the proposed system, the duty cycle of the dc/dc converter is directly adjusted by the outcome of the comparison between measurements of output power of WG. On the contrary of the wind velocity that changes severly by time, the power which is captured by WG, changes quite slowly, which is because of dynamic response of the interconnected generator system/ wind-turbine is slow.

Thus, the steepest ascent method is used to remove the problem of extracting the maximum output power of WG with regulating the duty cycle of the converter. This method conforms to the control law which is written below:

$$D_k = D_{k-1} + C_1 \frac{\Delta P_{k-1}}{\Delta D_{k-1}} \tag{15}$$

Where D_k is the duty cycle of iteration k and similarly, D_{k-1} is the duty cycle at iteration $k-1$. Morever, the value of duty cycle is limited between zero and one $(0 < D_k < 1)$ and the ratio of $\Delta P_{k-1} / \Delta D_{k-1}$ is the gradient of WG power in iteration $k-1$; and C_1 is the iteration change.

Due to show the feasibility of the proposed method and the power point movement of WG in the direction of its MPP for different wind velocity condition, existence of a single extreme point in function *P(D)* which coincides in MPPs of WG, will be enough for affirmation,as illustrated in Fig. 4. With regard to the WG power characteristic curves are represented in Fig. 4, it is clearly seen that at the points which maximum power is obtained:

$$\frac{dP}{d\Omega} = 0 \tag{16}$$

Where Ω is speed of the rotor in WG.

The above equation by implementation the chain rule rewritten as:

$$\frac{dP}{d\Omega} = \frac{dP}{dD} \cdot \frac{dD}{dV_{WG}} \cdot \frac{dV_{WG}}{d\Omega_e} \cdot \frac{d\Omega_e}{d\Omega} = 0 \tag{17}$$

Where the generator-phase-voltage angular speed and the rectifier output voltage level are represented by Ω_e and V_{WG} respectively.

About a buck-type dc/dc converter modeling, there is a relationship between the output (battery) voltage level, input voltage level and the duty ratio which is defined as below:

$$D = \frac{V_o}{V_{WG}} \rightarrow \frac{dD}{dV_{WG}} = -\frac{V_o}{V^2_{WG}} \neq 0 \quad (18)$$

Where the battery voltage level is represented by V_o .The relationship between speed of wind-turbine's rotor and generator speed is expressed as below:

$$\Omega_e = p \cdot \Omega \rightarrow \frac{d\Omega_e}{d\Omega} = p > 0 \quad (19)$$

Where the number of pole pairs is represented by p in generator. V_{WG} is proportional to the generator phase voltage V_{ph}. According to Fig. 5:

$$\frac{dV_{ph}}{d\Omega e} > 0 \quad (20)$$

$$\frac{dV_{WG}}{d\Omega_e} > 0 \quad (21)$$

With regard to (17)–(21), it leads to:

$$\frac{dP}{d\Omega} = 0 \Leftrightarrow \frac{dP}{dD} = 0 \quad (22)$$

Therefore, existence a single extreme point in the function $P(D)$ curve is approved. This point also coincides in the WG MPP, and adjusting the duty cycle of dc/dc converter under equation (15) leads to the power point movement of WG in the direction of its MPP for different wind velocity states. Fig. 6 illustrates the process of maximizing power. Owing to the adaptation of duty-cycle which tracks the direction of dP / dD , in the right side of the WG characteristic curve, the value of duty-cycle is augmented. The increased duty ratio in Buck converter will result in decreasing WG-rotor-speed and increasing power. Duty-cycle growth will be continued until the MPP is achieved.

If the process is begun at the point which is situated in the left side of characteristic curve, movement in the direction of dP / dD will be caused the duty-cycle becomes smaller, furthermore the speed of WG rotor increases. Finally convergence will be happened at the MPP.

The flowchart algorithm of the control system is illustrated in Fig. 7. The output voltage of battery is observed and when it gets to a level which is higher than threshold value, the battery stack will be protected from being overcharged if charging status is finished and the operation of MPPT is stopped. In order to specify the sign of the duty-cycle change ΔD, the WG output power at the current iteration is computed and contrasted to the same parameter at the previous one of the algorithm. Based on the comparison outcome, the sign of ΔD will be reversed or remain unchanged and subsequently the variation of PWM output duty cycle is applied properly, according to equation (15).

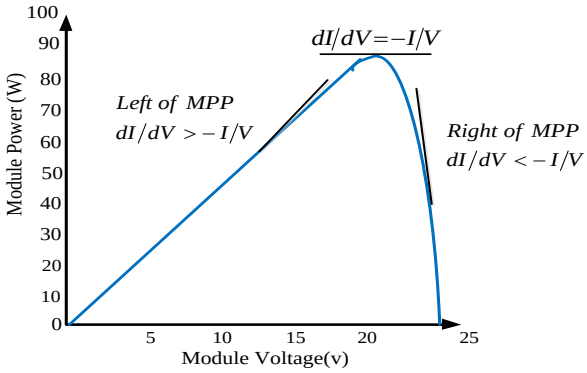

Fig. 6. MPP tracking process.

When adjusting the duty-cycle is finished, then the voltage level of WG must be measured. Two modes can be happened by the result, in the first one, it is below the maximum predefined value, the dummy load is separated from the circuit. In the other mode, it is upper than the maximum predefined value, so this load and the dc/dc converter is linked together in order to prevent the WG from over speeding. The hysteresis limits are set by the upper level and lower one predefined value. This is essential to stop the mentioned load from continuing its on/off state.

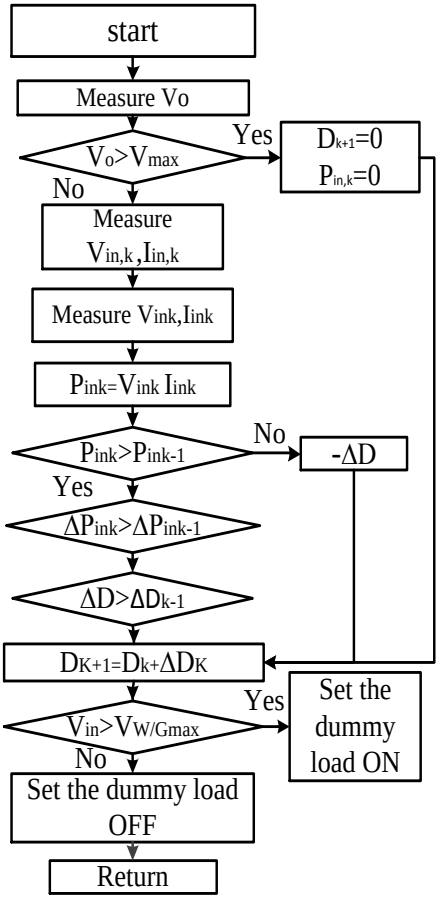

Fig. 7. MPPT process algorithm

5. Simulation Results

Table 1 lists the simulation parameters of BLDCM.

Table 1. Parameters of BLDCM.

Items	Specification
Type of inverter switches	MOSFET
Stator resistance	Bridge
Stator inductance	Rs=2.8750 Ω
Flux induced by	Ls=8.5e-3 H
magnets	0.175 W
Back emf flat area	120 degrees
Inertia	8.5e-3
Friction factor	1e-3
Pole pairs	4

Due to appraise the effectiveness of the proposed system, the wind velocity variation and the WG output power corresponding to that, are shown in Fig. 8(a) and (b). This point is clearly seen that the profile of WG output power imitates the wind speed changes. The rotor velocity and the coefficient of wind-turbine power are represented in Fig. 9(a) and (b). It is obvious that, the power coefficient comes rapidly near to its final value because the dynamic response is made better which results to less energy consumption. Also by implementing the proposed system, wind energy which can be obtained in the higher wind velocity variation, is increased. Fig. 10(a) and (b) show the corresponded generator current wave form and its spectra respectively. It is clearly seen that THD of the generator is diminished effectively.

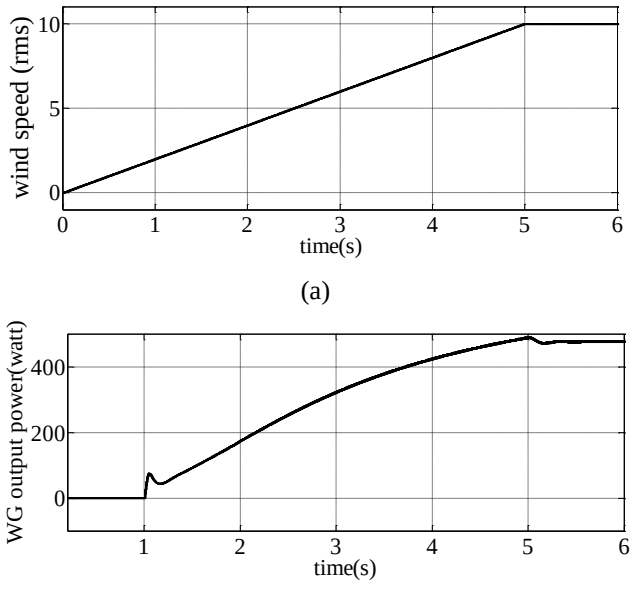

Fig. 8. (a) Wind speed, (b) WG output power, versus time.

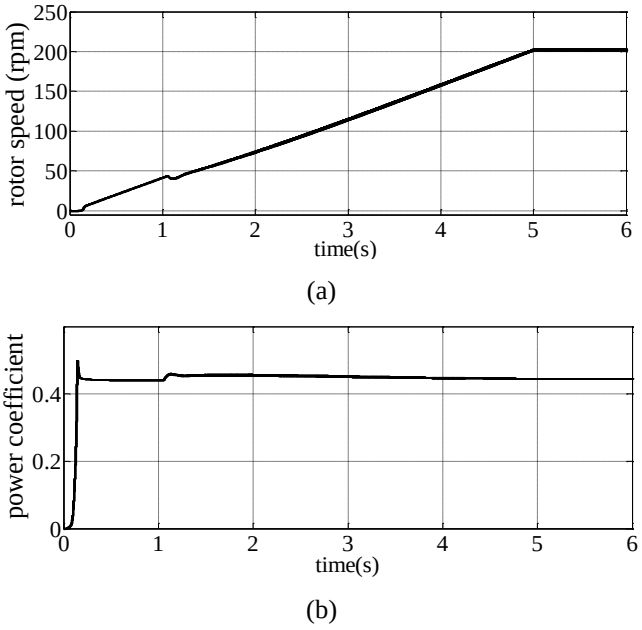

Fig. 9. (a) Rotor speed, (b) Power coefficient, versus time.

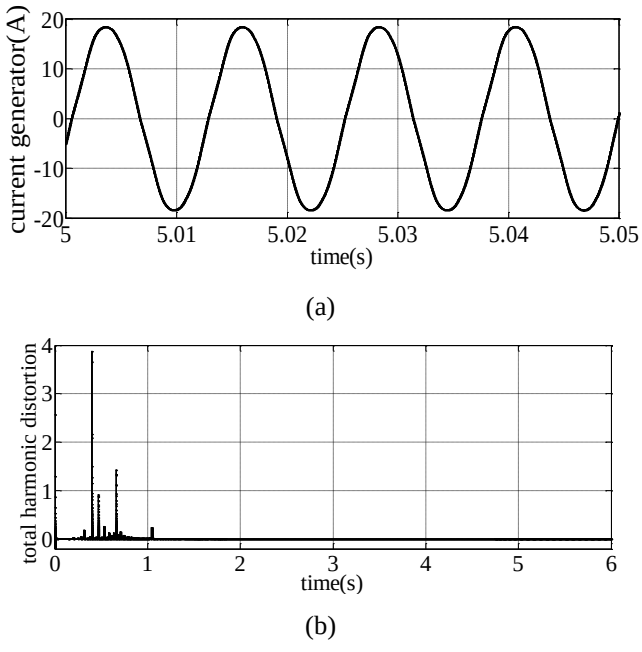

Fig. 10. (a) Generator current (b) THD of the generator.

Pi-filter is used for filtering the buck converter output. The output of the pi-filter is implemented to the three phase inverter and BLDCM is supplied by voltage type three phase inverter. Pulse width is 33% and output voltage level of Buck converter is 24 V. The applied pulses to BLDCM drive switches,are shown in Fig. 11.

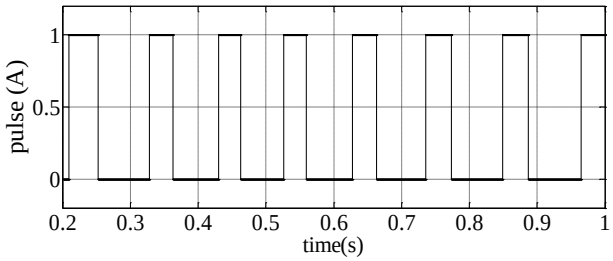

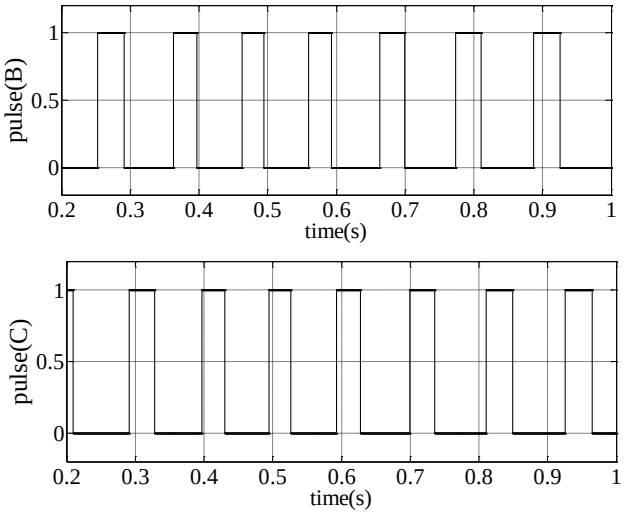

Fig.11. Triggering pulses

Voltage wave forms of inverter's legs are illustrated in Fig. 12. They are shifted by 120º. Three phase currents are given by BLDCM are shown in Fig. 13. The back EMFs are prepared for applying to the three phases of motor are shown in Fig. 14. Fig. 15 represents speed of rotor. As it can be seen, just before 1s motor reaches almost its final value due to fast dynamic response of motor and proper effect of the control system.

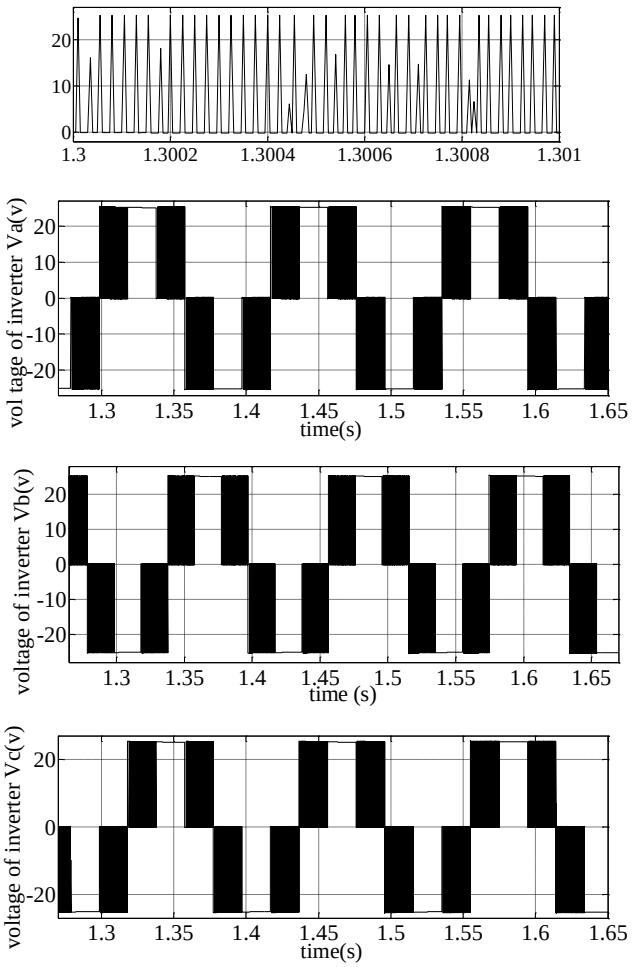

Fig. 12. Voltages of inverter.

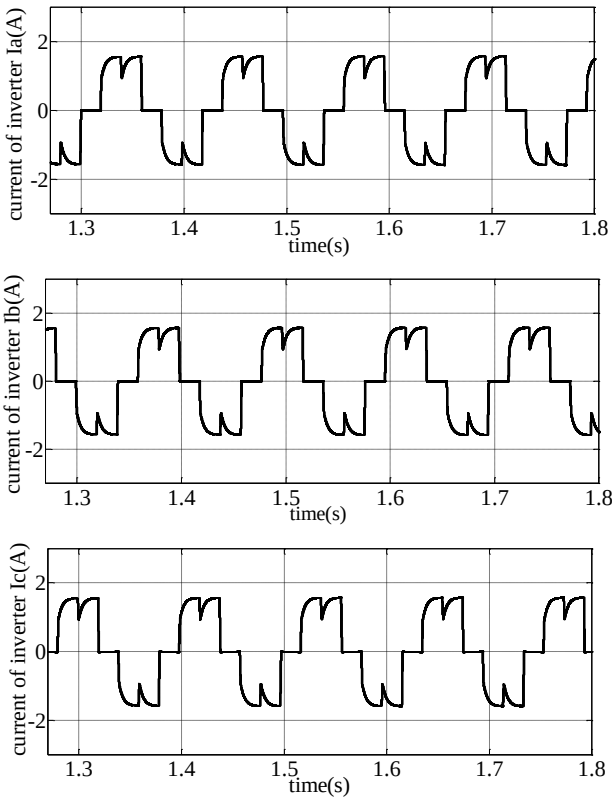

Fig. 13. Output currents of inverter.

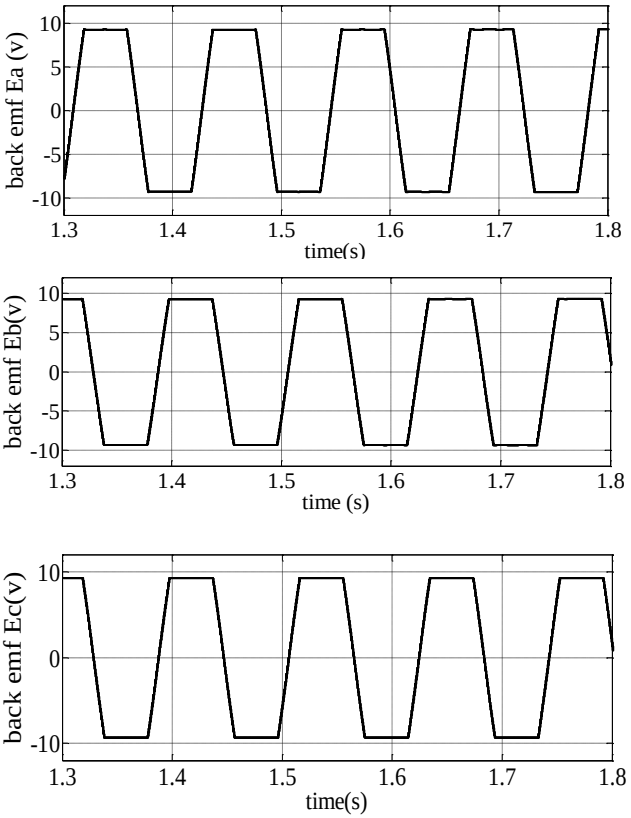

Fig. 14. Back EMF waveforms

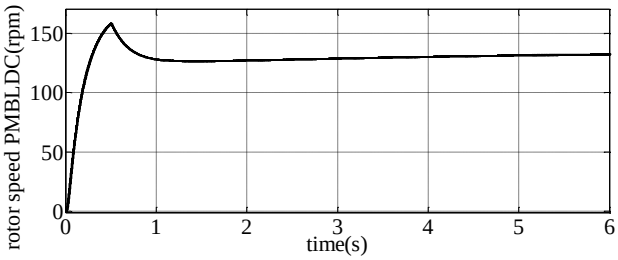

Fig. 15. Rotor speed of BLDCM.

6. Conclusion

In this paper a control system in order to drive a BLDCM which is used in electric vehicle applications, has been designed by usage of the mathematical model of the motor. Also a method for driving BLDCM using a WG and MPPT technique was proposed, including a high efficiency buck-type dc/dc converter and MPPT managing control unit. Due confirm performance of the proposed method and analysis the results, system modeling and simulating was performed by using MATLAB/SIMULINK software and the results was presented. Observing the figures, benefits of the proposed MPPT technique are as below:

I) Dynamic response was improved appropriately,

II) Wind speed sensor was not used,

III) The WG operated in variable velocity mode, so lower mechanical stress on the gears and shafts and less power fluctuation were occurred compared with constant velocity operation.

IV) Its applications were not restricted by the ratings of power of the dc/dc converter or WG wind and rotor-speed or. For reducing the input voltage to the required value, Buck converter was used.

References

[1] AWEA. (2007, Jul.). AWEA small wind turbine global market study 2007, in *The American Wind Energy Association Small Wind Systems* [Online]. Available: http://www.awea.org/smallwind/.

[2] A. M. knight and G. E. Peters, "Simple wind energy controller for an expanded operation range," *IEEE Trans. Energy Convers.*, vol. 20, no. 2, pp. 459–466, Jun. 2012.

[3] S. Morimoto, H. Nakayama, M. Sanada, and Y. Takeda, "Sensorless output maximization control for variable-speed wind generation system using IPMSG," *IEEE Trans. Ind. Appl.*, vol. 41, no. 1, pp. 60–67, Jan./Feb. 2005.

[4] K. Than and S. Islam, "Optimum control strategies in energy conversion of PMSG wind turbine system without mechanical sensors," *IEEE Trans. Energy Convers.*, vol. 19, no. 2, pp. 392–399, Jun. 2004.

[5] F. Valenciaga and P. F. Puleston, "Supervisor control for a stand-alone hybrid generation system using wind and photovoltaic energy," *IEEE Trans. Energy Convers.*, vol. 20, no. 2, pp. 398–405, Jun. 2005.

[6] E. Koutroulis and K. Kalaitzakis, "Design of a maximum power tracking system for wind-energy-conversion applications," *IEEE Trans. Ind. Electron.*, vol. 53, no. 2, pp. 486–494, Apr. 2006.

[7] R. Datta and V. T Ranganathan, "A method of tracking the peak power points for a variable speed wind energy conversion system," *IEEE Trans. Energy Convers.*, vol. 18, no. 1, pp. 163–168, Mar. 2009.

[8] Luk, P.C.K. and C.K. Lee, 1994. Efficient modeling for a brushless DC motor Drive. 20th International conference on Industrial Electronics, Control and Instrumentation, IECON'94, 1: 188-191.

[9] A. Sathyan, N. Milivojevic, Y. J. Lee, M. Krishnamurthy, and A. Emadi,"An FPGA-based novel digital PWM control scheme for BLDC motor drives," *IEEE Trans. Ind. Electron.*, vol. 56, no. 8, pp. 3040–3049, Aug. 2009.

[10] Atef, S.O. and Al-Mashakbeh, 2009. Proportional Integral and derivative control of brushless DC motor. Eur. J. Sci. Res., 35(2): 198-203.

[11] Byoung-Kuk, L., K. Tae-Hyung and J. Mehrdad Ehsani, 2001. On the feasibility of four-switch three phase BLDC motor drives for low cost commercial applications topology and control. IEEE Tran. Power Electron, APEC, 18(1): 428-433.

[12] Krishnan, R. and L. Shiyoung, 1997. PM brushless DC motor drive with a new power-converter topology. IEEE Tran. Indus. Appl., 33(4): 973-982.

[13] Krishnan, R., 2003. A Text Book on Electric Motor Drives, Modelling, Analysis and Control. Prentice Hall of India Pvt Ltd., New Delhi.

[14] Q. Wang and L.-C. Chang, "An intelligent maximum power extraction algorithm for inverter-based variable speed wind turbine systems," *IEEE Trans. Power Electron.*, vol. 19, no. 5, pp. 1242–1249, Sep. 2004.